MARS EQUATORIAL GLACIATION – COMPUTER AUTOMATION FOR IDENTIFICATION AND MORPHOMETRIC EXTRACTION OF CIRQUE GLACIERS ON MARS. J. M. Williams[1], L. A. Scuderi[1], T. P. McClanahan[2], M. E. Banks[2], D. M. H. Baker[2], [1]Dept. of Earth & Planetary Sci., Univ. of New Mexico, Albuquerque, NM 87131, USA, jwilliams4@unm.edu, [2]NASA Goddard Space Flight Center, Greenbelt, Maryland 20771, USA.

Introduction:

Identification and cataloging of glacial forms within the martian equatorial region has significant implications for past climate history and the possible equatorward redistribution of water ice. To understand these phenomena a Convolutional Neural Network (CNN) machine learning method was developed to conduct comparative planetology of cirque glaciers. Our CNN was trained on terrestrial cirque glaciers and then used to detect martian cirque glaciers [1] (Fig. 1). In addition to machine classification of martian cirques, this study aims to utilize automated morphometric extraction methods of identified cirque glaciers on Mars that can delineate cirques using digital elevation models (DEMs) based on a series of hydrological and morphological analyses [2]. Analysis of extracted morphometric information can provide insights into past climate sensitivity to changes in insolation in the equatorial region as well as to identify conditions that lead to a cryosphere capable of supporting glacial processes. Modern Mars, with its hyper-arid and tenuous atmosphere, is thought to be incapable of supporting glacial processes at low to mid latitudes [3, 4]. However, past martian climate (Hesperian/ early Amazonian periods) possibly could have supported an equatorward migration of the cryosphere. Further, changes in the martian atmosphere due to obliquity variations as recently as 5 million years ago could have supported glacial processes on the equatorial regions of Mars [5].

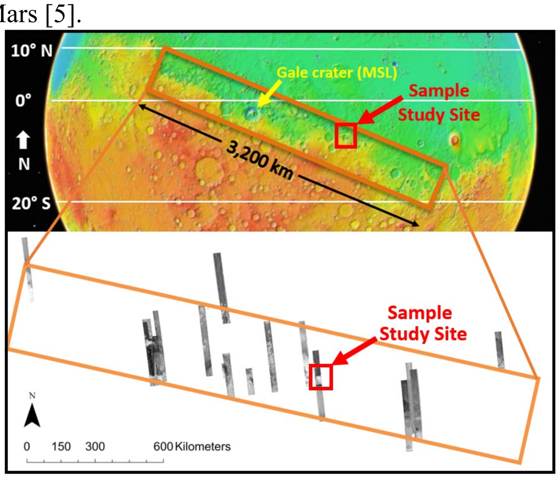

Fig. 1 Study area. **Top:** The 3,200 km extent of the martian equatorial dichotomy boundary (orange box). **Bottom:** DEMs derived from 17 CTX and HiRISE Stereopairs using the ISIS3 and ASP DEM pipelines. Image credit: NASA/JPL; Google Mars with MOLA topography; Williams, J.M.

Digital Elevation Model Production Approach

DEM data rather than orbital images were used for CNN training enabling the analysis of raw elevation. Where Context Camera (CTX) stereopairs were available the Integrated Software for Imagers and Spectrometers (ISIS3) and NASA Ames Stereo Pipeline (ASP) DEM pipelines [6] were used to create high quality DEMs (20m/pixel). ISIS3 is a format used by the USGS Planetary Cartography group to store and distribute planetary image data. The Geospatial Data Abstraction Library (GDAL) provides read, creation and update access to ISIS3 formatted image data. The NASA Ames Stereo Pipeline (ASP) is a suite of free and open-source automated geodesy and stereogrammetry tools designed for processing stereo images captured from satellites with and without accurate camera position information.

Machine Learning/Computer Automation

Convolutional Neural Network's (CNN) are a class of hierarchical neural network whose convolutional layers emulate the operation of neurons in the primary visual cortex of mammalian brains. A CNN is an artificial machine learning system that is primarily used to classify images, extract features, and localize objects from images [1, 7]. A CNN algorithm can identify critical morphometric information for object detection from DEM's more efficiently and dependably than manual extraction methods. Our model was trained using transfer learning from a Keras RetinaNet [8] CNN algorithm with a 50-layer CNN (ResNet50 backbone) as its core. Initial weights were from the default 500-object classes of the Common Objects in Context (COCO) dataset.

The CNN's internal weights are learned during training on a terrestrial cirque database. The trained CNN is then used to evaluate the martian topography and to identify candidate cirques. The backbone of a CNN refers to the feature extraction network that in essence processes the input data and creates a specific feature representation. Typically, in transfer learning a user can choose to freeze or unfreeze parts of the backbone of these large-scale prebuilt object detection, key-point detection, segmentation, and captioning datasets. This enables the user to keep the initial weights stable throughout training or, as in our case, allow the model to alter these initial weights as it optimizes (unfreezing). Unfreezing was done due to the robust training data set (terrestrial and martian) which allowed the model to fully optimize (increase the trainable parameters) to perform image classification.

For an initial pilot study, we used an off-the-shelf RetinaNet trained with over 20,000 terrestrial cirque forms and further trained with a small 50x50 km sample study site (Fig. 1). Initially, the sample study site yielded 27 cirque glacier identifications with over 3,200 false positive detections. False positives arose from DEM defects, tile edge errors and the detection of craters. False negatives arose from nested cirques (cirques within a cirque) (Fig. 2). Both false positives and false negatives were fed back into the training to further improve the performance, as measured by the mean average precision (mAP) [1].

Discussion and Conclusions:

Other than our pilot study there are no automatic identification and morphometric extractions for glacial forms on Mars [1]. Here we expand our initial study and apply a convolutional neural network that was originally trained on a large global distribution of terrestrial cirque glaciers [7].

Equatorial glacial forms documented in previous studies [5, 9, 10] are noted as having similar features to terrestrial analogs. However, little in the way of empirical morphometric analysis of these features exists. This study adds supporting evidence to the hypothesis that the equatorial region of Mars was modified by glacial processes.

Our study found that the cirque glacier forms within the study area were significantly larger than their terrestrial counterparts. While the length, width, perimeter and area of martian cirques were generally larger (50%), martian cirque headwall heights were consistently smaller (25%) than their terrestrial equivalents. This could be due to the weaker gravitational force on Mars (3.721 m/s²) influencing glacial flow as well as other impacts of martian climate, such as cold based glaciation during cirque formation or possible reworking and subsequent deflation of the cirque forms by aeolian processes [1].

If cirque-like alcoves identified in the initial study were created through glacial processes, the timing of their creation is still poorly understood. The equatorial cirques could be ancient, and the relative timing of their creation could be as old as the Hesperian to Amazonian transition (~3 Ga). However, they could be created due to the equatorward redistribution of the martian cryosphere during more recent periods of high obliquity oscillations.

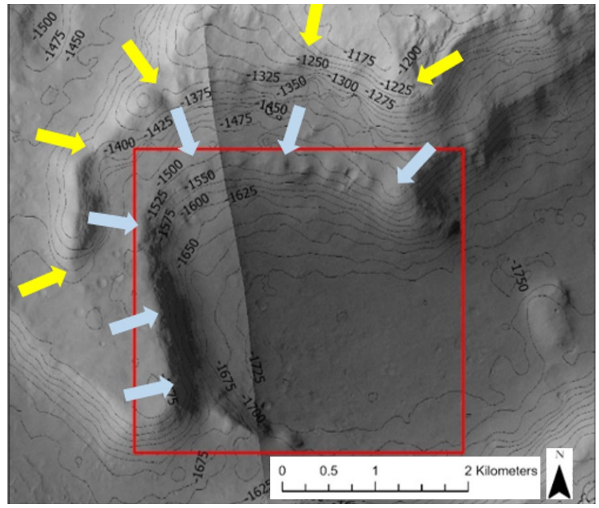

Fig. 2 Nested cirque example within the initial sample study area. Blue arrows indicate edge of detected cirque form. Yellow arrows indicate the edge of an outer cirque form initially missed by the algorithm. Center of image 8° 7'2.53"S, 152°40'21.86"E.

Future work will include automated detection of craters to remove false positives and for crater counting. This will then be aggregated and added to a global cirque database for statistical analysis. Automation of the DEM production using the ASP and ISIS3 pipelines to produce this database should be done on a global scale where coverage is available. CTX stereo pair derived DEMs could then be analyzed using our RetinaNet CNN procedure to detect and identify cirque glacier features, to extract geomorphic data and add to a global cirque database. This enhanced dataset will allow a better understanding of both past martian climate and its geomorphic evolution from the Hesperian through the Amazonian.

References:

[1] Williams, J.M., (2022) *AGU Fall Meeting Abstracts.* [2] Li, Y. and Z. Zhao, (2022) *Geomorph.,* 398: p. 108059. [3] Conway, S.J., et al., (2018) *Geomorph.,* 318: p. 26-57. [4] Dickson, J.L., et al., (2008) *Geol.* 36(5). [5] Williams, J.M., et al., (2022) *Rem. Sen.* 14(8): p. 1887. [6] Beyer, R.A., et al., (2018) *Earth and Space Sci.,* 5(9): p. 537-548. [7] Scuderi, L.A. and T. Nagle-McNaughton, (2022) *Phys. Geog.,* 43(1): p. 24-51. [8] https://github.com/fizer/kerasretinanet [9] Davila, A.F., et al., (2013) *Geol.,* 41(7): p. 755-758 [10] Head, J.W., et al., (2006) *EPSL,* 241(3-4): p. 663-671.